

# HIGH ASPECT-RATIO 3D MICROSTRUCTURES VIA NEAR-FIELD ELECTROSPINNING FOR ENERGY STORAGE APPLICATIONS

Guoxi Luo<sup>1,2</sup>, Kwok Siong Teh<sup>2,3</sup>, Xining Zang<sup>2</sup>, Dezhi Wu<sup>2,4</sup>, Zhiyu Wen<sup>1\*</sup>, and Liwei Lin<sup>2\*</sup>

<sup>1</sup>College of Optoelectronic Engineering, Chongqing University, Chongqing, CHINA

<sup>2</sup>Department of Mechanical Engineering, University of California at Berkeley, Berkeley, CA, USA

<sup>3</sup>School of Engineering, San Francisco State University, San Francisco, CA, USA

<sup>4</sup>School of Aerospace Engineering, Xiamen University, Xiamen, CHINA

## ABSTRACT

High-aspect-ratio, three dimensional (3D) microstructures have been constructed by a direct-write method via self-aligned near-field electrospinning process. Using papers as the collectors, the process enables both design and fabrication of a variety of 3D structures, such as walls, grids and other configurations based on layer-by-layer deposition of electrospun micro/nano fibers. Afterwards, these fabricated polymeric structures can be mechanically separated from the paper substrate for various applications. In this work, we have successfully fabricated 20-layer, ca. 100  $\mu\text{m}$  in thickness,  $2 \times 2 \text{ cm}^2$  3D grid-structures made of PVDF (Polyvinylidene fluoride) electrospun fibers. After a coating process using the dip-and-dry process in the CNT (carbon nanotube) ink, conductive and flexible electrodes made of CNT coated polymer grid-structures have been demonstrated and assembled as a micro-supercapacitor.

## INTRODUCTION

Electrospinning is well-known as a simple, versatile, and flexible process that utilizes high electrostatic forces to produce continuous micro/nano fibers [1-4]. A wide range of fibers made of different polymers [5-6], polymer with embedded nanoparticles [7-9], metals [10] and ceramics [11] have been successfully made previously. Applications for electrospun fibers include filtration [12], biomedicine [13], sensing [14], energy [15-16], and electronics [17]. Experimentally, four major components are required for electrospinning: a high voltage supply; a syringe; a spinneret; and a collector. When a high voltage is applied to the polymer solution in the syringe/spinneret, a droplet is formed and the electrostatic force may overcome the surface tension to eject a liquid jet toward the ground collector. The charged jet first goes through a stable region, then a bending instability [18] region for the stretching and drying processes. The solidified fibers are deposited on the collector. As a result, electrospun fibers are generally formed as randomly oriented nonwoven mats.

Suppressing bending instability to obtain well-aligned and highly ordered electrospun fibrous meshes has been an important direction in the research of electrospinning techniques. Among different reported schemes, near-field electrospinning (NFES) with short spinneret-to-collector distance (0.5 ~ 3 mm) utilizes the stable region of the ejected liquid jet for controllable fiber depositions to make arbitrary 2D patterns [19, 20]. In this paper, we report a direct-write 3D electrospinning technique to construct controllable high aspect-ratio microstructures in a continuous, self-aligned, fiber-by-fiber manner on paper

collectors. This out-of-plane electrospinning process could act as an additive 3D fabrication technique that bridges the gap between electrospinning and 3D fabrication to enable new electrospinning applications.

In this paper, a free-standing grid-structure made of stacked PVDF fibers has been constructed. By using a dip-coating process in the CNT ink, the grid-structure is coated with a CNT layer as a 3D macroporous, flexible, and conductive electrode for applications in solid-state micro-supercapacitors.

## SETUP AND MATERIALS

### Experimental Details

Figure 1 illustrates the schematic setup of this 3D fabrication technique that synergistically combines several concepts. First, this method is based on NFES, whose spinneret-to-collector distance ranges from 500  $\mu\text{m}$  to 3 mm to realize the accurate depositions of electrospun fibers. Second, a programmable  $x$ - $y$  translational motion stage is utilized to directly deposit the electrospun fibers in a pre-designed path to stack fibers repeatedly. In addition, a  $z$ -axis manual linear motion stage is used to preserve the spinneret-to-fiber distance. Finally, the key in achieving this 3D electrospinning is the use of a printing paper placed on the top of the grounded conductive plate. Generally speaking, electrospun fibers using the NFES process remain wet after being deposited on the collector because of the short spinneret-to-collector distance which prevents the complete evaporation of solvent [20]. Once deposited on porous papers, residual solvents in fibers can infiltrate the paper substrate and enhance the charge transfer to the ground plate through the paper network as illustrated in the inset of figure 1. As such, the grounded fibers become electrical poles to attract subsequent fiber depositions in a self-aligned manner on top of each other.

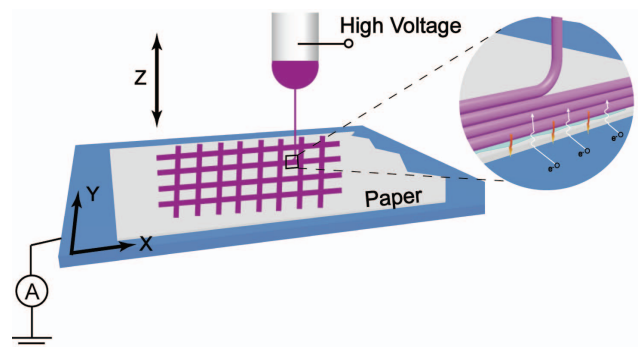


Figure 1: Schematic diagram of the 3D electrospinning process with the mechanism of self-aligned fiber-by-fiber stacking. A paper collector is placed on top of a conductive ground plate and the charges on the deposited

*fibers can be conducted through the paper to the ground. As such, the deposited fibers become the ground electrodes on top of the paper to attract and stack newly deposited fibers.*

All experiments were conducted under the room temperature and one atmospheric pressure environment. The typical electrospinning parameters are: 30G as the spinneret size, 10 ~ 90 mm/s as the speed of motion stage, 1.0 ~ 1.8 kV as the applied voltage, and 0.5 ~ 2.0 mm as the spinneret-to-collector distance for specific patterns and structures to be constructed.

### Materials Preparation

Polyvinylidene fluoride (PVDF,  $M_w = 534\ 000$ ), polyvinyl alcohol (PVA,  $M_w = 90\ 000$ ), dimethyl sulfoxide (DMSO), acetone, anionic surfactant Capstone® FS-66, single-walled carbon nanotube (SWNT), sodium dodecylbenzenesulfonate (SDBS), and phosphoric acid were all purchased from Sigma-Aldrich (United States) without further purification or modification. The polymer solution is critical to the success of the 3D electrospinning process. In general, 2.1 g PVDF in powder form was added into 5 g acetone and stirred for 30 minutes using a magnetic stirrer to obtain a uniform suspension. Afterwards, 5g DMSO and 0.5 g Capstone® FS-66 surfactant were added and the mixture was stirred for one hour as the PVDF solution. The surfactant caused foaming during the stirring process, therefore the final solution needed to stand for another hour to get rid the foams. All solution containers were sealed with Parafilm to minimize evaporation.

For the CNTs ink, 1.0 g CNTs powder and 1.0 g SDBS were added into 100 mL water and sonicated for 1 hour. The PVA/phosphoric acid electrolyte was made by adding 1.0 g PVA powder and 1.0 g phosphoric acid into 8.0 ml of DI water with stirring on an 85°C hot plate until the mixture became a clear and glue-like gel.

## RESULTS AND DISCUSSION

### Micro-Wall Structures

Figure 2(a) shows the oblique view scanning electron micrograph (SEM) of a free-standing, straight micro-wall structure fabricated by the 3D electrospinning technique with 50 layers of electrospun PVDF fibers. The inset illustrates that the fibers are stacked consistently and without deviating from the pre-designed path. This wall is ca. 100  $\mu\text{m}$  in height and ca. 5  $\mu\text{m}$  in width with a high aspect-ratio about 20. Figure 2(b) shows a different micro-wall fabricated by stacking 50 layers of electrospun fibers. Compared with figure 2(a), this structure was fabricated with the same electrospinning parameters except that the motion speed of the  $x$ - $y$  stage was lowered from 50 to 30 mm/s. The lower motion speed resulted in better solidifications of individual fibers before contacting with other fibers and less stacking accuracy. On the other hand, excessive motion speed ( $> 90$  mm/s) can cause the fracture of electrospun fibers and termination of the electrospinning process. Figures 2(c) and (d) show top view SEM photos of the arrays of wall structures with 20-layer of electrospun fibers with gaps of ca. 100  $\mu\text{m}$  and

ca. 50  $\mu\text{m}$ , respectively. The gap distance was designed and constructed using the programmable motion stage. Occasionally, electrospun fibers may go out of the intended paths due to the electrostatic interferences from adjacent walls and other disturbances during the process.

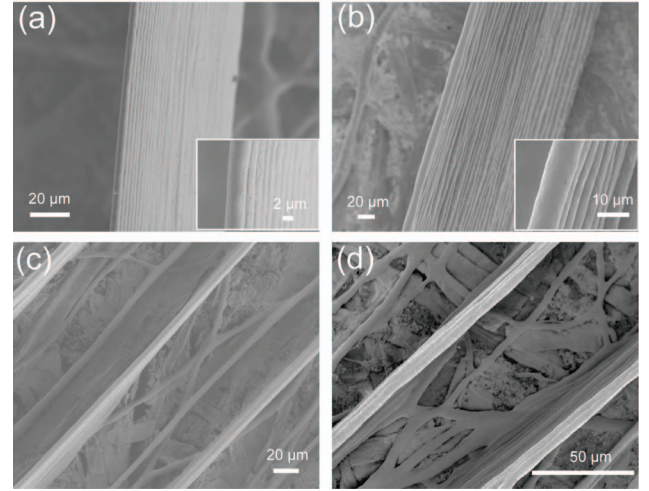


Figure 2: (a) The oblique view SEM photo of a free-standing micro-wall with 50-layers of electrospun fibers stacked on top of each other. The electrospinning parameters are as follows: applied voltage at 1.5 kV, motion stage speed of 50 mm/s, and spinneret-to-collector distance of 1 mm. (b) A micro-wall structure fabricated with the same parameters in (a) except for the lower motion stage speed at 30 mm/s. (c) An array of the wall structures with a gap of ca. 100  $\mu\text{m}$  using the fabrication process in (a). (d) Another array of wall structures with a gap of ca. 50  $\mu\text{m}$  using the same process parameters in (c).

Figures 3(a) and (b) record the width of the micro wall structures — equivalent to the diameter of a single fiber — under the process parameters of applied voltage at 1.5 kV, motion stage speed at 50 mm/s, solution concentration at 21 wt% and spinneret-to-collector distance at 1mm when motion speed and applied voltage are altered for each graph, respectively. It is found that the width of the free-standing micro wall structure is increased from ca. 3.0  $\mu\text{m}$  to ca. 10.0  $\mu\text{m}$  as the motion speed of the  $x$ - $y$  stage is reduced from 90 to 10 mm/s because of the reduction of mechanical drawing. On the other hand, wall width decreases from ca. 5.5  $\mu\text{m}$  to ca. 4.0  $\mu\text{m}$  when the applied voltage is increased from 1.0 to 1.8 kV because of higher electrostatic stretching force.

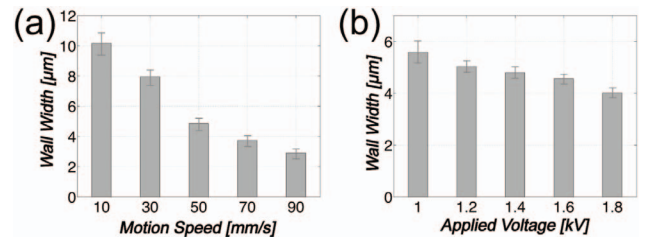


Figure 3: The dependence of the wall width on (a) the motion speed of the  $x$ - $y$  stage, and (b) the applied voltage.

### 3D Grid Structures



A grid-structure made of 20-layer of electrospun PVDF fibers in an area of  $2 \times 2 \text{ cm}^2$  on a paper substrate has been produced as shown in figure 4(a). The whole fabrication process took ca. 50 minutes for a total fiber length of ca. 80 meters with fiber diameter of ca.  $8 \mu\text{m}$ . The SEM image in figure 4(b) reveals the details of the structure with twenty fibers successively electrospun on top of another and a lateral grid pitch of ca.  $200 \mu\text{m}$ .

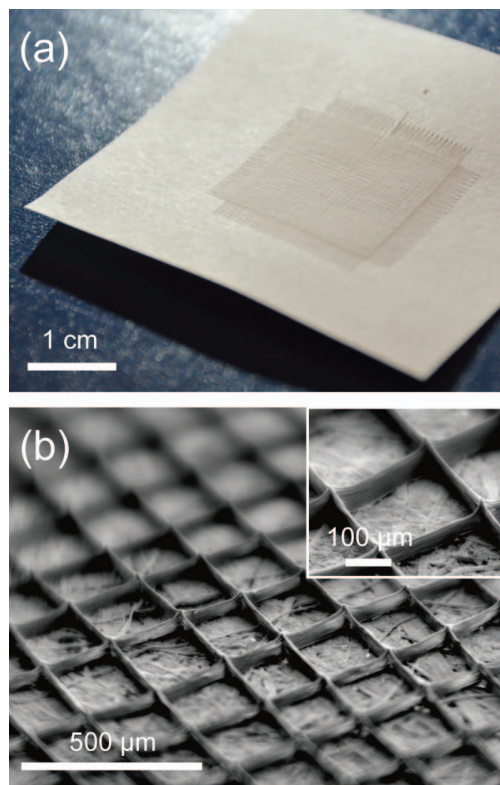


Figure 4: (a) An optical photo of a 3D grid structure on the paper substrate. The electrospinning parameters are: applied voltage at 1.5 kV, motion stage speed at 25 mm/s, and spinneret-to-collector distance at 1 mm. (b) SEM image showing twenty layers of electrospun fibers are stacked vertically for the construction of this 3D grid structure with a lateral grid pitch of ca.  $200 \mu\text{m}$ .

#### Application: 3D Electrodes for Supercapacitor

The fabricated polymeric 3D structures can be mechanically detached from the paper substrate for various potential applications. In this work, the grid structures are detached and dipped into CNTs ink as shown in figure 5(a), followed by a drying process to coat the surface with a dense layer of CNTs as shown in figure 5(b) with a measured conductivity of ca. 850 S/m. The structure maintains the original shape after the dip-and-dry process, highlighting the structural integrity with strong adhesion between fibers as well as CNTs. Figure 5(c) is measured Raman spectrum showing signature wavenumbers of both PVDF and CNT. The inset shows the close-up SEM image at the cross-over location of the fabricated grid structure.

The 3D conductive grid electrode was attached to a steel conductive plate and coated with the PVA/phosphoric acid as both the electrolyte and separator material. Two of these electrodes were then assembled

face-to-face to make a solid-state micro-supercapacitor as shown in figure 5 (d). The assembly was dried in room temperature for 12 hours. As a reference, two sheets of steel were assembled with about 1mm-thick PVA/phosphoric acid and CNTs in between as a control cell under the same process. The inset of figure 5(d) shows the CNTs coating on the steel plate is not uniform due to the agglomeration of CNTs and the coffee ring effect. It is found that the CNT film on top of the steel plate can be easily washed away by water due to the weak adhesion force between the steel and CNTs.

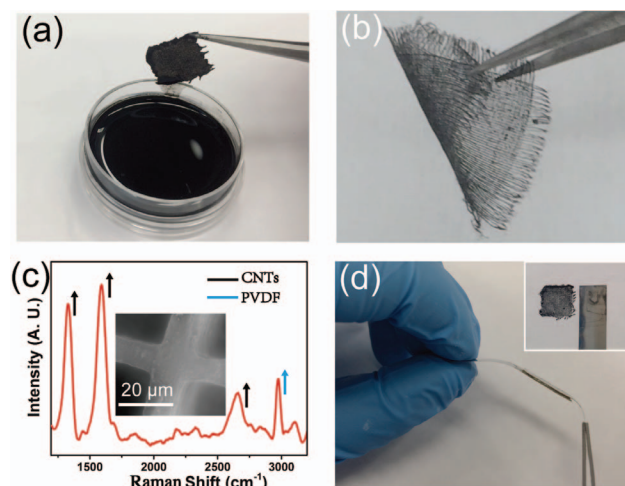


Figure 5: (a) The dip-coating process in the CNT ink solution; (b) a flexible 3D electrodes made of the 3D grid-shape PVDF electrospun fibers after a dense coating of CNTs; (c) the Raman spectrum analysis showing signs of both PVDF and CNT with inset showing the cross-over location of the electrospun grid structure; (d) a solid-state micro-supercapacitor made of two grid-structure coated with CNTs and steel plate current collectors; the inset showing the PVDF grid structure (left) and steel plate (right) after the dip coating and drying process.

The supercapacitor performance is characterized by a Gamry Reference 600 potentiostat. Figure 6(a) compares the cyclic voltammetric (C-V) curves of a cell with the 3D grid-structure electrodes and a control cell. The estimated capacitance of the prototype with the 3D grid-structure is  $3.2 \text{ mF/cm}^2$ , which is about 25 times larger than that of the control cell. The enhancement in capacitance could be attributed to: (i) the 3D grid-structure with larger surface area compared with the 2D flat electrodes; (ii) higher van der Waals force interaction between CNT and polymer for better adhesions resulting in larger amount of CNTs on the 3D grid-structure [21]; and (iii) high surface charges on the electrospun polymer fibers in the electrospinning process to attract and enhance CNT adhesion. Specifically, the anionic surfactant SDBS was used for the uniformity of CNTs in the solution. The electrostatic attraction between the electrospun fibers and CNTs-SDBS can lead to a much denser layer of CNTs coating for high surface area and high capacitance. Figure 6(b) shows the C-V curves of the same prototype system using the 3D grid-structure under different scanning rates. The curves show that the current density is almost proportional to the

scan rate, which is a typical behavior of a well-performed supercapacitor.

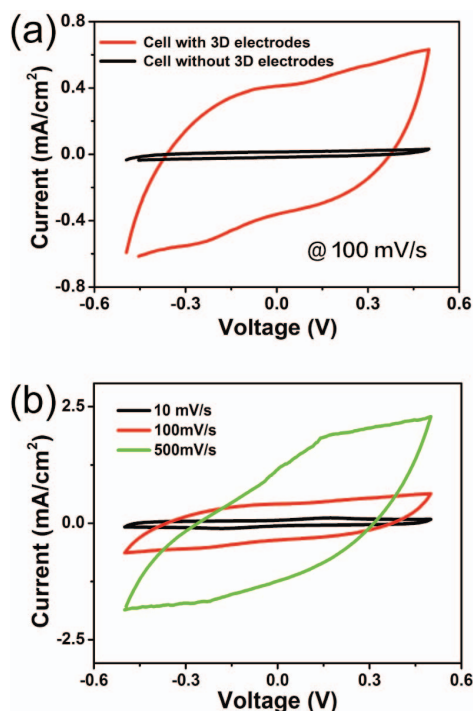


Figure 6: C-V results of prototype micro-supercapacitors: (a) with and without the 3D grid-structure in the electrode; and (b) results from different scanning rates.

## CONCLUSION

Near-field electrospinning has been applied to make high aspect-ratio, 3D microstructures on paper substrates. This process enables orderly depositions and fiber-by-fiber stacking of micro/nano fibers to fabricated structures such as micro-walls and 3D grids in a controllable, self-aligned manner. In addition, the fabricated 3D structures can be conveniently detached from the paper substrate for other process treatments and applications. In this work, a simple dipping process in the CNT ink has been used to coat the electrospun 3D grid structures with CNTs. The resulting structures have been utilized and demonstrated to make electrodes in solid-state supercapacitors.

## ACKNOWLEDGEMENTS

The authors thank Mr. Caiwei Shen for valuable discussions. Prof. K. S. Teh was funded by a sabbatical award from the San Francisco State University and Mr. G. Luo was funded by the China Scholarship Council (CSC).

## REFERENCES

- [1] D. H. Reneker, I. Chun, "Nanometre Diameter Fibers of Polymer, Produced by Electrospinning", *Nanotechnology*, vol. 7, pp. 216-223, 1996.
- [2] D. Li, Y. Xia, "Electrospinning of Nanofibers: Reinventing the Wheel?", *Adv. Mater.*, vol. 16, pp. 1151-1170, 2004.
- [3] Y. Dzenis, "Spinning Continuous Fibers for Nanotechnology", *Science*, vol. 304, pp. 1917-1919, 2004.
- [4] C. -L. Zhang, S. -H. Yu, "Nanoparticles Meet Electrospinning: Recent Advance and Future Prospect", *Chem. Soc. Rev.*, vol. 43, pp. 4423-4448, 2014.
- [5] W. K. Son, J. H. Youk, T. S. Lee, W. H. Park, "The Effects of Solution Properties and Polyelectrolyte on Electrospinning of Ultrafine Poly(ethylene oxide) Fibers", *Polymer*, vol. 45, pp. 2959-2966, 2004.
- [6] A. Baji, Y. W. Mai, Q. Li, Y. Liu, "Electrospinning Induced Ferroelectricity in Poly(vinylidene fluoride) Fibers", *Nanoscale*, vol. 3, pp. 3068-3071, 2011.
- [7] F. Ko, Y. Gogotsi, A. Ali, N. Naguib, H. Ye, G. L. Yang, C. Li, P. Willis, "Electrospinning of Continuous Carbon Nanotube-Filled Nanofiber Yarns", *Adv. Mater.*, vol. 15, pp. 1161-1165, 2003.
- [8] D. He, B. Hu, Q. F. Yao, K. Wang, S. H. Yu, "Large-Scale Synthesis of Flexible Free-Standing SERS Substrates with High Sensitivity: Electrospun PVA Nanofibers Embedded with Controlled Alignment of Silver Nanoparticles", *ACS Nano*, vol. 12, pp. 3993-4002, 2009.
- [9] B. Dong, M. E. Smith, G. E. Wnek, "Encapsulation of Multiple Biological Compounds Within a Single Electrospun Fiber", *Small*, vol. 5, pp. 1508-1512, 2009.
- [10] H. Wu, L. Hu, M. W. Rowell, D. Kong, J. J. Cha, J. R. McDonough, J. Zhu, Y. Yang, M. D. McGehee, Y. Cui, "Electrospun Metal Nanofiber Webs as High-Performance Transparent Electrode", *Nano Lett.*, vol. 10, pp. 4242-4248, 2010.
- [11] R. Ramaseshan, S. Sundarajan, R. Jose, S. Ramakrishna, "Nanostructured Ceramics by Electrospinning", *Appl. Phys. Lett.*, vol. 102, pp. 111101, 2007.
- [12] R. Gopal, S. Kaur, Z. Ma, C. Chan, S. Ramakrishna, T. Matsuura, "Electrospun Nanofibrous Filtration Membrane", *J. Membrane Sci.*, vol. 281, pp. 581-586, 2006.
- [13] J. W. Li, C. T. Laurencin, E. J. Caterson, R. S. Tuan, F. K. Ko, "Electrospun Nanofibrous Structures: A Novel Scaffold for Tissue Engineering", *J. Biomed. Res. A*, vol. 60, pp. 613-621, 2002.
- [14] B. Ding, M. Wang, X. Wang, J. Yu, G. Sun, "Electrospun Nanomaterials for Ultrasensitive Sensors", *Materials Today*, vol. 13, pp. 16-27, 2010.
- [15] C. Chang, V. H. Tran, J. Wang, Y. K. Fuh, L. Lin, "Direct-Write Piezoelectric Polymeric Nanogenerator with High Energy Conversion Efficiency", *Nano Lett.*, vol. 10, pp. 726-731, 2010.
- [16] F. Zhang, C. Yuan, J. Zhu, J. Wang, "Flexible Films Derived from Electrospun Carbon Nanofibers Incorporated with  $\text{Co}_3\text{O}_4$  Hollow Nanoparticles as Self-Supported for Electrochemical Capacitor", *Adv. Func. Mater.*, vol. 23, pp. 3909-3915, 2013.
- [17] S. -Y. Min, T. -S. Kim, B. J. Kim, H. Cho, Y. -Y. Noh, H. Yang, J. H. Cho, T. -W. Lee, "Large-Scale Organic Nanowire Lithography and Electronics", *Nat. Commun.*, vol. 4, pp. 1773, 2013.
- [18] Y. M. Shin, M. M. Hohman, M. P. Brenner, G. C. Rutledge, "Experimental Characterization of Electrospinning: the Electrically Forced Jet and Instabilities", *Polymer*, vol. 42, pp. 09955-09967, 2001.
- [19] D. Sun, C. Chang, S. Li, L. Lin, "Near-field Electrospinning", *Nano Lett.*, vol. 6, pp. 839-842, 2006.
- [20] C. Chang, K. Limkraisiri, L. Lin, "Continuous Near-field Electrospinning for large area deposition of orderly nanofiber patterns", *Appl. Phys. Lett.*, vol. 93, pp. 123111, 2008.
- [21] L. Hu, M. Pasta, F. L. Mantia, L. Cui, S. Jeong, H. D. Deshazer, J. W. Choi, S. M. Han, Y. Cui, "Stretchable, Porous, and Conductive Energy Textiles", *Nano Lett.*, vol. 10, pp. 708-714, 2010.

## CONTACT

\*Liwei Lin, tel: +1-510-6435495; lwlin@berkeley.edu  
\*Zhiyu Wen, tel: +86-023-65104131; wzy@cqu.edu.cn